J. Indian Inst. Sci.
A Multidisciplinary Reviews Journal
ISSN: 0970-4140 Coden-JIISAD

REVIEW ARTICLE

Recent Advances in Single Particle Cryo-electron Microscopy and Cryo-electron Tomography to Determine the Structures of Biological Macromolecules

Moumita Dutta[*]

Abstract | A detailed three-dimensional structure of macromolecular assemblies is necessary to understand their function which in turn helps to understand life. Cryo-electron microscopy (cryo-EM) is a powerful method for structural studies of a wide range of different sizes biological macromolecules and their complexes. Cryo-EM has three different imaging modalities based on specimen and imaging condition: single particle analysis (SPA), cryo-electron tomography (cryo-ET) plus sub-tomogram averaging (STA)/sub-volume averaging (SVA) and electron diffraction. Richard Henderson and Nigel Unwin revealed the structure of the first membrane protein bacteriorhodopsin from electron diffraction data. This led to the beginning of understanding molecular structures of biomolecules in three-dimension. Soon after that, a unique vitrification method of biomolecules has been successfully developed by Jacques Dubochet more than two decades ago. Ordered 2D array or biomolecules with internal symmetry have long been considered for structure determination to achieve better resolution. But structure calculation by electron microscopy was at that time known as blobology to others due to low resolution (image with less information) compared to X-ray. Since then imaging and software technologies have steadily improved and after 2013, with the development and success of direct detectors, the world witnessed a resolution revolution in cryo-EM. Now cryo-EM more specifically single particle analysis has achieved the resolution at which protein complex can be studied at near-atomic level. This once a highly skilled and difficult technique has now become a widely accepted biophysical technique in structural biology. Here the two methods of cryo-EM (SPA and cryo-ET) and recent studies are reviewed.

Keywords: *Cryo-electron microscopy, Single particle analysis, Cryo-electron tomography, Sub-tomogram averaging, Direct detector, Defocus, Resolution, Dose symmetry, Conformational heterogeneity*

Vitrification: It is a cryo-preservation method when water from the liquid state directly transformed to amorphous non-crystalline or glass-like form without turning into crystalline form.

Low resolution image: Images with small number of pixels and less information and less detail.

[1] *Division of Electron Microscopy, Indian Council of Medical Research-National Institute of Cholera and Enteric Diseases, P-33, C.I.T. Road, Scheme XM, Beleghata, Kolkata, West Bengal 700010, India.*
**moumita.dutta@icmr.gov.in*

1 Introduction

Structural biology is expanding widely due to technological advances that developed alongside molecular biology during early in the twentieth century. Structural biology is capable of solving structures to understand the associated function and deducing a molecular model. Structural biology initially developed based on two techniques: X-ray crystallography and nuclear magnetic resonance (NMR). At the same time ultrastructure analysis of cells and tissues using electron microscopy was flourishing in the field of cell biology.

Springer IISc Press

SNR (signal-to-noise ratio): This is a measure used to compare the level of signal output to the level of background noise.

During 1950s negative staining was developed as a working technique for biological samples. Negatively stained images of large, stable and homogeneous proteins will undergo averaging technique to increase the signal-to-noise ratio (SNR) and thus allow further details of the molecule to be visualized.[1] For symmetrical particles such as icosahedral viruses, computational aligning and averaging of several negatively stained particles achieved better resolution of the three-dimensional reconstruction calculated.[2] But due to distortion and artifacts which are integral part of negative staining, the resolution of structures was limited to 25 Å. Richard Henderson with Nigel Unwin studied the first structure of membrane protein bacteriorhodopsin by electron diffraction pattern and imaging.[3] The low dose electron micrographs were analyzed and 3D map at 7 Å resolution was calculated from 2D projections based on central section theorem by Aaron Klug's group.[4] Henderson's theory of replacing water with glucose solution to preserve bacteriorhodopsin structure did not work well for other membrane proteins. During that time sample freezing in liquid nitrogen was applied by Taylor and Glaeser to protect from radiation damage.[5] However, ice crystals were formed which destroyed the signals coming out of the specimen. To overcome the problem of crystalline ice Swiss scientist Jacques Dubochet first introduced the method of vitrification (rapid plunging of sample into very low-temperature cryogen such as liquid ethane at −190 °C to form non-crystalline glass like vitreous ice) of water-based unstained biological samples in their native state.[6, 7] These samples are of low contrast, but high-resolution. Thereafter, the word cryo has been added with electron microscopy and a new wing of structural biology has developed namely, cryo-electron microscopy or electron cryo-microscopy. This wing of structural biology has steadily improved in last 10 years with rapid advances in microscope design with improved stability, introducing field emission gun, constant power lens system, Cs/Cc corrector, energy filter, phase plate technology, automatic, and high throughput data collection[8,9], user friendly and sophisticated software[10, 11], image processing algorithms and most importantly development of direct detectors[12, 13]. In the era of resolution revolution, cryo-EM is capable of doing high-resolution structures which were exclusive to X-ray crystallography and NMR spectroscopy.[14] The flowchart in Fig. 1 shows a comparison of X-ray crystallography and cryo-EM methods.

In 2015 cryo-EM was declared as the method of the year by Nature group of publishers [15], but the foundation was laid decades ago. As an obvious result, the Noble prize in Chemistry in 2017 had been awarded to Jacques Dubochet, Richard Henderson and Joachim Frank for their pioneering works in the development of cryo-EM as a structure determination technique. In recent years, single particle analysis (SPA) and cryo-electron tomography (cryo-ET) with improved and simplified technologies have set new horizons for

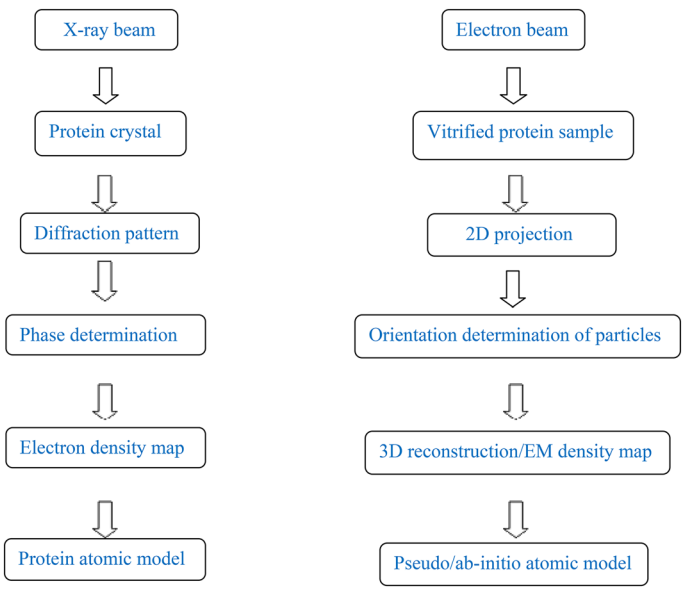

Figure 1: X-ray crystallography vs cryo-EM.

their usefulness in structural biology and many other fields. The basic procedure of the two techniques of cryo-EM is reviewed in the following sections with reference to the current advances and their contribution in recent studies.

2 Technological Advancements

For the remarkable advancement of cryo-EM structural studies of biomolecules and macromolecular complexes, a number of newly developed technologies have been implemented. In this section that technological progress is discussed.

2.1 Direct Detector Device (DDD) and Aligning Movie Frame

The transmission electron microscopy classic imaging technique involves indirect detection of electrons. At first, the primary electrons are converted to photons by a scintillator, which is coupled to the charged-coupled device (CCD) sensor through a fiber-optic coupling. In comparison, direct detection is a better alternative based on complementary metal–oxide–semiconductor (CMOS) technology using electrons directly on the thin layered DDD sensor to generate image (Fig. 2). The direct detector has the practical advantage over CCD in terms of high-detective quantum efficiency (DQE) and readout speed[16]. It has two different modes: integrating and counting mode. Direct detectors allow collecting images in movie mode with several raw frames for each image and all of them have usable information because of their high frame rates. While processing data the frames could be aligned to perform motion correction using available software program motioncor[13], motioncor2[17] and unblur[18] which dramatically reduces beam-induced motion of imaged molecules and stage drift and thereby enhances data quality significantly. All direct detector cameras can operate at moderate to high frame rates.

2.2 Phase Plate Technology

Low dose imaging technique is used to take cryo images with low signal-to-noise ratio (SNR), but without radiation damage. Therefore, contrast enhancement is needed to visualize the molecules in cryo-EM using defocus phase contrast and sacrificing high-resolution information. This limitation motivated researchers to develop a better contrast enhancement technique of cryo images. A few decades ago, in light microscopy, a similar problem was solved by Zernike by placing a phase plate in the diffraction plane for pure phase imaging[19]. A similar method was tried by researchers in transmission electron microscope, but they were not very successful during initial days.[20] The first TEM phase plate that showed promising results was known as Zernike phase plate (ZPP).[21] In this phase plate a thin film, able to retard phase by 90° with a central hole of 1 μm, is placed in the back focal plane or diffraction plane of the objective lens. Thereby shifting the phase of the scattered electrons and their interference with the unscattered electrons at image plane results in amplitude contrast. But this technique has also some practical disadvantages: small lifespan of the phase plate, centering the beam into the small

DQE (detective quantum efficiency): DQE actually means how effectively a camera can detect an electron or produce an image with high signal-to-noise ratio.

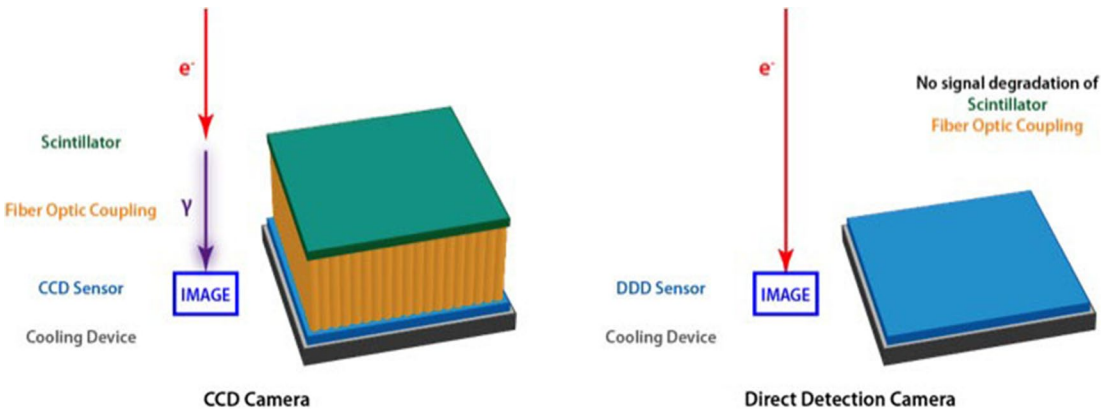

Figure 2: Working principle of direct detector device (DDD). Conventional digital cameras (left) with a charged-coupled device (CCD) uses a scintillator to convert primary electron into photons to be detected by an imaging sensor. In this process, a signal is degraded by scintillator and fiber-optic coupling whereas direct detection camera (right) detects electron directly in the microscope. [Courtesy of Benjamin Bammes, Direct Electron LP, San Diego, CA].

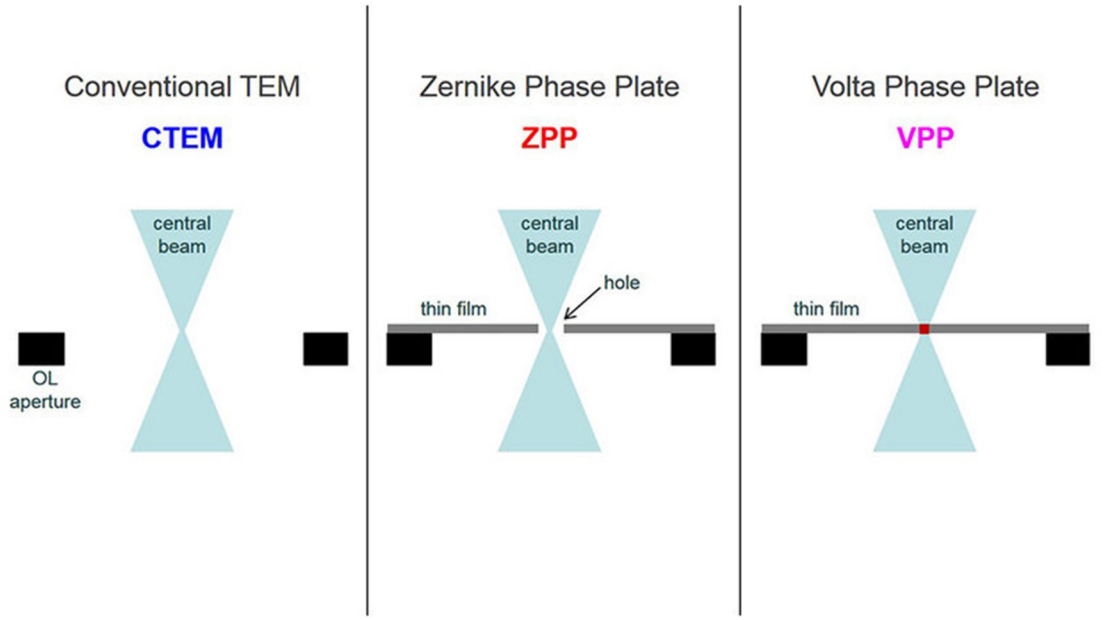

Figure 3: Design of thin film phase plates (middle and right). The most recent is the Volta phase plate suitable for automatic data acquisition because it does not have any central hole rather a large open area to use multiple phase plates. [Courtesy of Dr. Radostin Danev, Max Planck Institute of Biochemistry, Department of Molecular Structural Biology, Germany].

hole of the phase plate and fringe artifacts. This lead to the development of a simply designed phase plate known as Volta phase plate (VPP) with a thin amorphous carbon film constantly heated to ~ 250 °C.[22] Compared to ZPP there is no central hole and the phase shift occurs on-the-fly, the higher longevity of the plate and there are no fringe artifacts (Fig. 3).

2.3 Energy Filters

When a beam of high-energy electrons passes through a thin sample some electrons remain unchanged while passing through the sample, but some of them interact with the sample and scattered both elastically and inelastically. The inelastically scattered electrons lose energy and change their momentum and result in adding only noise to the image. Energy filters have a slit in the middle to stop the inelastically scattered electrons by allowing only elastically scattered and unhindered electrons to pass through the slit to improve the quality of the image. Energy-filtered transmission electron microscope (EFTEM) uses two types of energy filters: one is in-column and the other one is bottom mount[23]. In terms of design, the in-column filter works better with its symmetric design compared to bottom mount which is prone to distort the image but recent upgradation of bottom mount energy filters has shown less geometric distortion and along with direct detectors enhances the contrast and successfully applied to study vitrified cells and giant viruses.

Inelastically scattered electrons: These are electron that lost some of their kinetic energy and contributes noise to an image. For example, thick specimens result in more inelastically scattered electrons.

Elastically scattered electrons: These are coherent electrons contributes signal for image formation.

2.4 Sample Support Film

Recent developments of direct detector camera have allowed cryo-EM to be considered as an alternative technique to determine protein structure which was previously approached only with X-ray crystallography. But even after the success of direct detector, the fragile nature of biological samples and beam-induced motion of support film impedes regular achievement of high-resolution structure beyond 2 Å. There are continuous efforts to push the resolution for cryo-EM structures by optimizing sample preparation technique.[24]

Exposure of electron beam creates an unrecoverable deformation in the carbon support film that induces image blurring and difficulties in aligning 2D images. In 2014 MRC-LMB scientist Lori Passmore and colleagues addressed this problem using hydrogen plasma-treated graphene support film to reduce the beam-induced motion and better sample distribution.[25] Later they worked on the same problem using gold support film (Fig. 4) and found a further reduction in motion or almost eliminate motion.[26] The proposed gold support grid is straightforward to

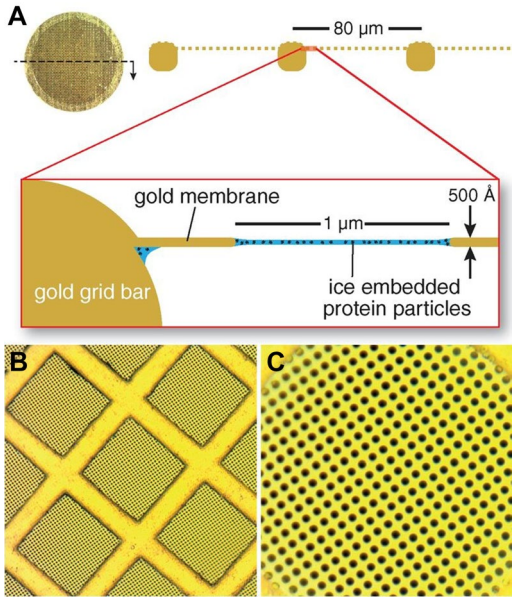

Figure 4: Ultrastable substrate design. The ultrastable gold support comprises a 3-mm diameter disk of gold mesh **a** where ~ 500 Å thick layer of gold foil with a regular array of micrometer-sized holes is suspended across the square openings in the mesh (diagramed along the section indicated). After application of an aqueous protein sample and plunge freezing at ~ 80 K, each hole contains a thin film of protein particles embedded in vitrified ice. **a**–**c** Optical micrographs of the gold grid at low, medium, and high magnification, respectively, each hole is 1.2 µm in diameter and sets the scale for **b** and **c**. Reproduced from [26] with permission obtained through RightsLink.

manufacture than graphene grids. Additionally, they pointed out gold grids can generate better images not only in high-end microscopes with new generation detectors, but also in the old ones.

2.5 Sample Preparation and Standardization

Sample preparation is a key step towards a successful high-resolution reconstruction in cryo-EM. Grid choice (200–400 mesh), treatment of grids (glow-discharged) and support films also contribute significantly. A typical protocol is as follows: a small volume (3–5 µl) of highly concentrated sample is applied to a treated grid for about a minute, extra liquid is blotted to leave a thin film of liquid containing sample, and then rapidly freezing at a rate of $\sim 10^6$ °C/s by plunging into liquid ethane or ethane–propane mixture cooled by liquid nitrogen. In this procedure, the water in, and surrounding the specimen will be fixed in a vitreous state with the protein embedded in a different orientation. However, every sample is different and needs standardization to provide ideal cryo-EM data. During initial days plunging devices built in-house were used, but these devices were often unable to reproduce results when temperature and humidity in the room and grid batches were changed.[27] Therefore, commercial plunge-freezing instruments were made by different companies (Leica, Gatan, and FEI) with more controlled environment and automation to increase the productivity.

2.6 Advanced Microscope Design and Data Collection

Most of the new generation microscope comes with multi specimen autoloader to load up to 12 grids and screen them continuously for 5 days without any contamination and manipulation of each grid. Specimen stage stability has been increased by removing the side entry holder in new design and specimen cartridge remain inside the microscope column. Automated alignment procedure allows the microscope to maintain optimal settings for SPA or tomography experiments. Remote operation of almost all function including apertures has prompted to make automated data collection software for high throughput cryo-TEM. Available software in cryo-EM are Leginon,[9] SerialEM,[28] UCSF-Image4,[29] FEI EPU/Tomography4, JEOL JADAS. With the continuous run, every day at least 3–5 TB data will be generated depending on the movie frames. For tomography data collection it could be higher and also time-consuming. John Briggs and colleagues have proposed a new tilt series data collection scheme to maintain the high-resolution information by collecting low tilt angle images first without any damage due to prolonged exposure[30].

Cryo-electron tomography is predominantly used to study pleomorphic cellular structures and often suffers from the thickness of the sample (> 5000 Å).[31] To overcome the problem of sample thickness two different approaches were developed successfully. Cryo-EM of vitreous sections (CEMOVIS) that requires vitrification of biological material and cutting it into ultrathin sections, which are observed in the vitrified state, and later combined with electron tomography.[32] The other method is cryo-focused ion beam (cryo-FIB) milling that enables cryo-ET to analyze native cells and tissues thinner than 3000 Å.[33] But often unique and transient structures are lost while thinning samples and introduces another method known as correlative light and electron microscopy (CLEM).[34]

3 Single Particle Analysis

For decades, researchers have used X-ray crystallography and NMR to solve structures of biomolecular complexes at high-resolution. However, solving membrane protein structures by X-ray crystallography is extremely difficult. Similarly, NMR is capable of determining structures of the only small protein. As an alternative, cryo-EM single particle analysis was introduced during 70–80 s and radiation sensitivity of biomolecules was also discovered.[35] At that time, low dose imaging technique was proposed[36] and image processing and analysis of low SNR low dose cryo-EM data of macromolecules were developed.[37] But recent progress in EM optics, stage stability, data collection software, energy filter, phase plate technology and successful implementation of direct detector cameras has brought single particle analysis in the forefront as a routine approach in structural biology laboratories[38, 39]. Soon after the discovery of direct detector cameras in 2013, an exponential growth has been observed in the deposition of cryo-EM derived high-resolution structures at EMDB (www.emdatabank.org) within few years[40].

A typical workflow of high-resolution cryo-EM SPA illustrating sample preparation and data analysis is shown in Fig. 5. The advantage of single particle cryo-EM is that it is capable of solving the structure of non-crystalline macromolecules and their assemblies. Single particle averaging method was first showed by Joachim Frank for determining the correct orientation of the same molecule in multiple views and averaging of those views[43]. In single particle data collection, low dose procedure is used to take high-resolution images to minimize the radiation damage and images are taken at a slightly under focus to increase phase contrast. CTF modifies the amplitude of an EM image and, therefore, has a direct relation with defocus. Therefore, contrast transfer function (CTF) correction is routinely done in single particle analysis computationally using the software. Thousands of identical particles in random orientation are imaged from frozen samples and then computationally averaged together to

CTF correction: CTF is a function that modulates the amplitude and phases of the electron diffraction pattern of the object formed by the objective lens while image formation in bright field electron microscopy. The point where it first crosses the spatial frequency axis called first zero or point resolution of the microscope and where the CTF dampened to zero is called the information limit of the microscope.

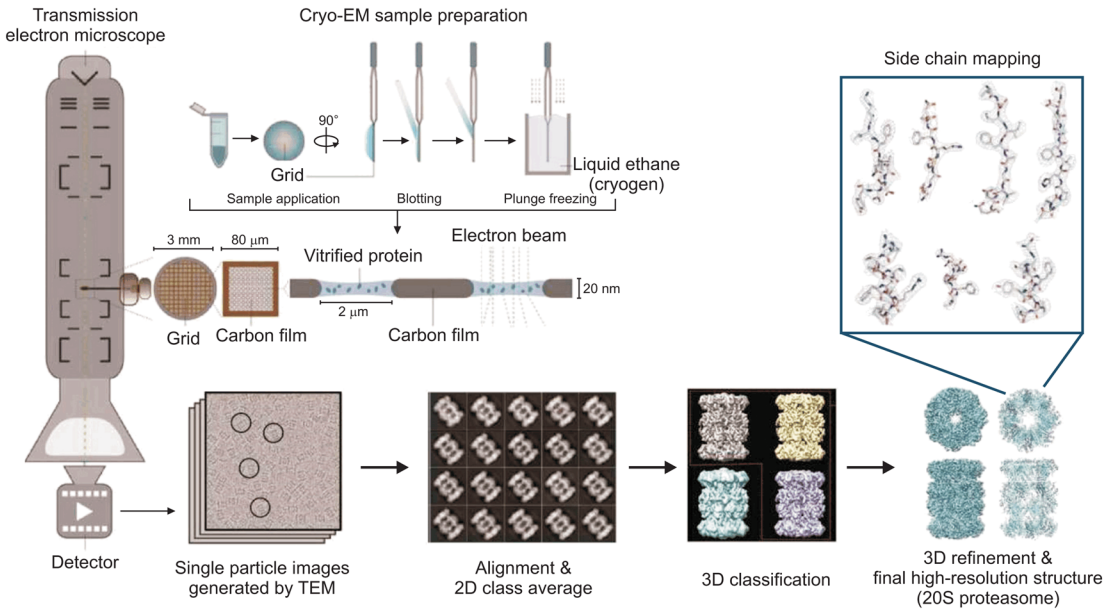

Figure 5: Cryo-electron microscopy (EM) Workflow. This figure is reproduced with kind permission from Dr. Ho Min Kim, based on the review.[41] Briefly, purified sample is applied to the grid and then vitrified in liquid ethane. Particles embedded in the thin ice with random orientations are imaged at low dose imaging condition using a cryo-TEM. Image processing software to do motion and contrast transfer function (CTF) correction were applied. Individual particles are then selected and aligned to calculate two-dimensional (2D) class average. Three-dimensional (3D) classification and further iterative refinement of 3D reconstruction will finally calculate the high-resolution cryo-EM structure (Here a 3 Å cryo-EM structure of archaea 20S proteasome processed with RELION 2.0 is shown) [42].

increase the SNR dramatically. Next, orientation searches and aligning of the projections are done iteratively and a three-dimensional (3D) map is reconstructed. Another important cryo-EM structure determination technique is by helical reconstruction. In this method, a small segment of helices is treated as single particle and imposing the correct helical symmetry a high-resolution structure of helical viruses and flexible filaments can be calculated. Compared to single particle analysis, multiple copies of the same repetitive, asymmetrical unit with fixed relative orientation need to be averaged[44].

An ideal single particle specimen has to be homogeneous. But heterogeneity in the sample may appear from conformational variation and flexibility. Advanced image processing algorithms are capable of classifying and averaging heterogeneous sample[10]. However, heterogeneity in sample sometimes restricts the structure determination to negative stain EM analysis. Single particle cryo-EM has expanded in last 10 years and entered the realm of crystallography to take the challenge in solving small, heterogeneous and difficult to crystallize molecules. To date, a wide range of dynamic biomolecules and macromolecular complexes including many important membrane proteins have been solved by single particle cryo-EM because of its advantage of data collection without any crystals. Electron crystallography has long been used to study many important membrane proteins such as bacteriorhodopsin, aquaporin, tubulin and several others. But in this golden era of single particle cryo-EM many biologically important membrane proteins are successfully studied.[45, 46] Some notable works using advanced SPA technique have been reported at remarkably high-resolution (~2–3 Å) including revisited structures and some small size proteins.[47–56] Figure 6 shows the gallery of few examples of recently solved high-resolution structures of broad range molecular weight of biomolecules.

A perfect area to image for single particle analysis is where the holes are covered fully with identical particles distributed closely, but not touching each other and in multiple orientations. High-quality image acquisition is another important step in single particle analysis which includes alignment of the microscope, selection of right aperture, magnification, defocus setting, spot size, direct alignment, and optimum dose calculation. Low resolution maps calculated by single particle analysis are usually validated by fitting atomic model (if available) as a rigid body into the density map [57] which also determines the handedness. But recent progress has made flexible fitting as a better choice for high-resolution cryo-EM data.[58] Assessment of resolution to detect overfitting and validity of model increases the reliability of functional interpretation. A method was proposed to obtain the absolute hand of the cryo-EM map and improve the accuracy of particle orientation and contrast loss, thus improving the quality of the resulting map.[59]

The growing field of single particle cryo-EM with more advanced hardware or software will be able to solve much more structure of proteins and their complexes, but there are still certain issues that will impede the resolution to go beyond 2 Å. Air–water interface causing denaturation of fragile macromolecules in a thin layer of vitreous ice is a major problem. Other barriers are conformational heterogeneity, the thickness of sample, beam-induced motion, charging effect and radiation damage. Better sample preparation technique and more stable and homogeneous sample are needed to go beyond 1.8 Å using a modern cryo-EM platform.

4 Cryo-electron Tomography and Sub-tomogram Averaging

In spite of the success in obtaining atomic-level details of many important proteins and protein complexes, single particle analysis has some limitation. It is unable to study macromolecules within cells, proteins that are difficult to purify and biomolecules that exhibit continuous conformational flexibility.[60] Generally, the isolated and purified molecules hardly reveal the biological functions performed by them in a native environment. Cryo-ET has been developed to link high-resolution electron microscopy and structure–function relation. Using cryo-ET we can visualize a protein in situ within its native environment compromising with the resolution. In other words, cryo-ET is bridging a gap between light microscopy and in vitro structure determination techniques. In recent years with the development of direct detector camera, energy filters and a phase plate, the resolution of cryo tomograms has improved drastically. Cryo-ET is applicable to get the three-dimensional structure of complex objects such as whole cells, cellular organelles, molecular machines, pleomorphic viruses.

Data collection in tomography is much more challenging than single particle analysis as the dose distribution in the whole set of images is crucial to avoid radiation damage in the field of imaging. Figure 7 illustrates a general workflow of cryo-ET where a series of images are collected

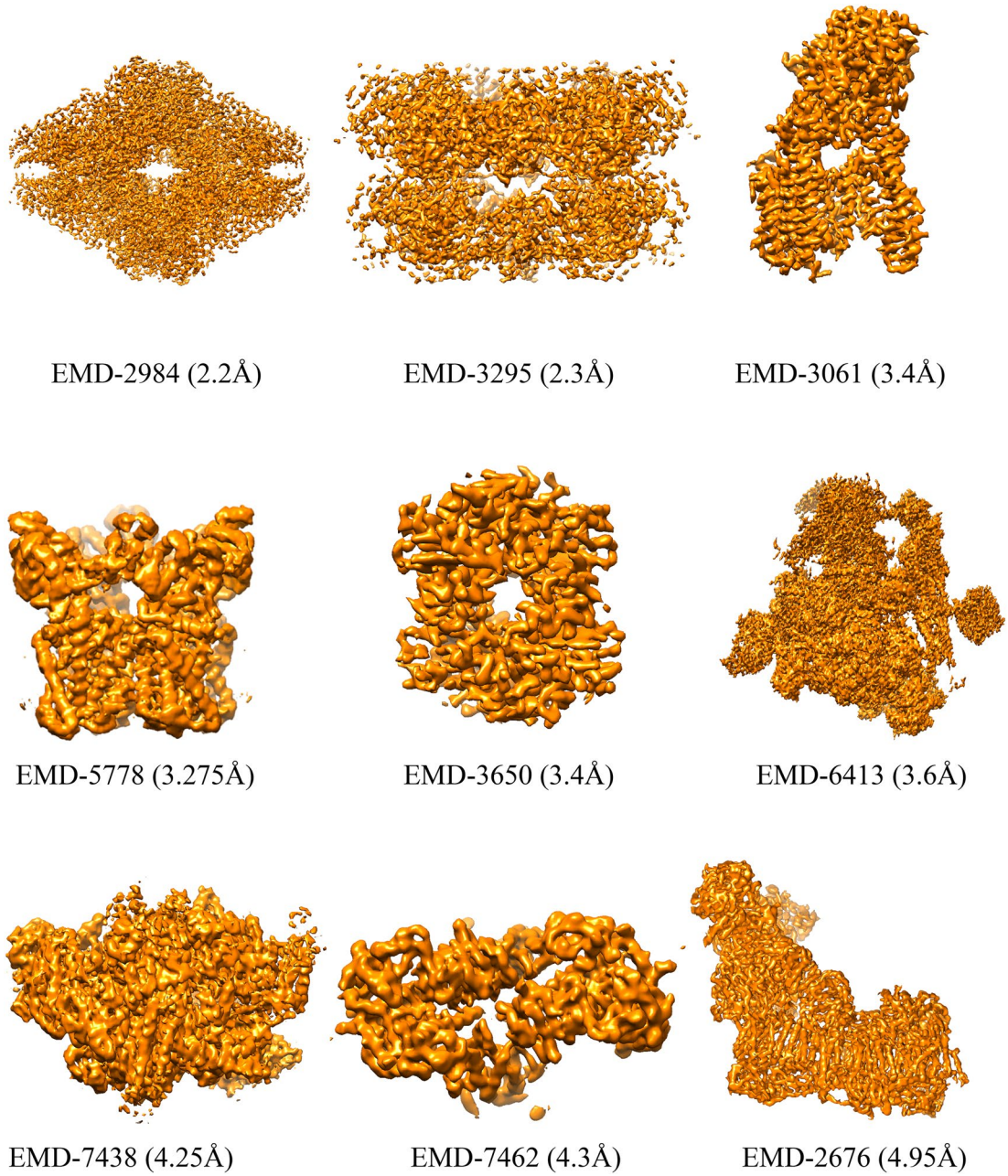

Figure 6: Representative biomolecules of a wide range of molecular weight recently solved by cryo-EM at near-atomic resolution. EM database number and resolution of the reconstruction are indicated below the respective map. First row: (L) beta-galactosidase,[47] (M) human p97 bound UPCDC30245 inhibitor,[48] (R) human gamma-secretase complex.[50] Middle row: (L) TRPV1 ion channel,[51] (M) human hemoglobin,[52] (R) yeast spliceosome,[53] bottom row: (L) E. coli RNAP sigma70 holoenzyme and promoter DNA complex,[54] Insulin Receptor-Insulin Complex,[55] (R) mammalian respiratory complex I [56].

for each specimen area by tilting the specimen stage through a range of angles $\pm 60°$, usually about a single axis and the whole series of images is called a tilt series. High cumulative electron dose (80–120 e/A^2) needed to obtain optimum contrast in each image of a tilt series for better alignment. After that, the collected tilt series are computationally reconstructed into a 3D tomogram showing the macromolecules with more clarity compared to individual 2D images. Gold fiducial markers are used in tomogram reconstruction to precisely orient each image in a tilt series.[62] But sometimes the gold particles are also shown to undergo independent beam-induced

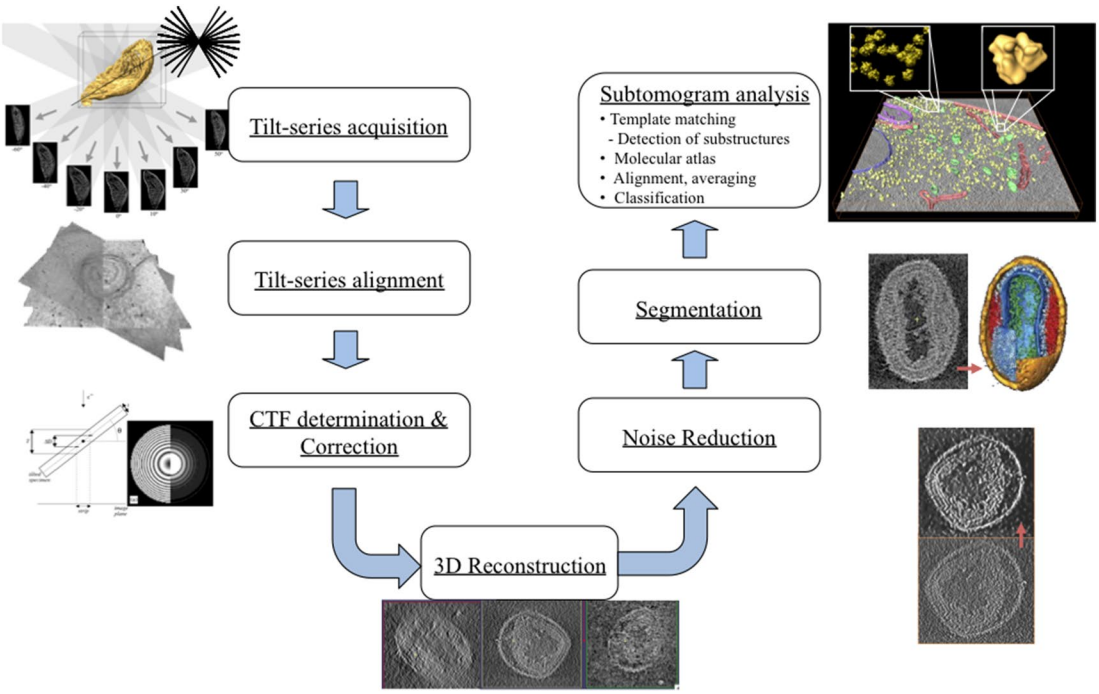

Figure 7: Image processing workflow in structural studies by cryo-ET. This figure kindly provided by Dr. J. J. Fernandez, based on the review.[61] Reproduced from https://sites.google.com/site/3demimageprocessing/research_projects/comet with permission of the author. 2D images are acquired at different tilt angles around a single axis and aligned. In high-resolution structural studies, CTF is determined and correction is done. Next, the tomographic reconstruction computationally combines the aligned images to get the 3D volume or tomogram. After that, the tomogram is subjected to denoising with preservation of details. Next, the tomogram is segmented into structural components. Finally, if repetitive sub-volumes are present those will be extracted for sub-volume averaging. This analysis includes 3D alignment and averaging of the sub-tomograms to obtain a high-resolution map and quantitative analysis of the distribution of the sub-volumes are done.

Denoising: It is a signal processing method to remove noise from an image and to preserve the useful information.

motion that reduces the quality of reconstruction and also the strong artifacts caused by gold fiducials obscure features. Therefore, fiducial less alignments have been developed.[63, 64]

Like SPA data collection, defocus is applied to enhance the contrast of the imaging area during tilt series. Since defocus is directly related to the specimen height in the microscope column, tomography samples produce a variable CTF across the imaging plane due to tilting. As a result, correction of CTF in tomography data is far more complicated than SPA cryo-EM. Before direct detector and other CTF correcting software,[65–67] the resolution was limited between 30–60 Å or more depending on sample and imaging parameters. But recently with the technical advancements, the resolution has improved rapidly and lies between 8 and 20 Å. However, this resolution is anisotropic due to the restricted tilt angle data collection. The mechanical constraints of the specimen holder do not allow to tilt $-90°$ to $+90°$ range. As a result, the tomograms are stretched in the direction of the electron beam and this effect is called missing wedge due to the shape of the missing information in Fourier space. In general, the 3D volume or tomogram is quite noisy and subjected to noise reduction while preserving the structural details. After that, segmentation is usually done in the denoised tomogram to visualize the structural components and to understand their spatial relationship.

Segmentation: This is a computational process to partition a digital image into several segments to simplify the image into a more useful representation to better analyze the data.

There is another specialized technique associated with cryo-ET applicable on the aligned and denoised tomogram, based on the principle of single particle analysis, which is also gaining popularity with the improvement in instrument and automated data collection, known as sub-volume averaging or sub-tomogram averaging. It can be applied to calculate 3D map of an object present in the tomogram in multiple copies and scattered at a different orientation. The resolution will be much higher than the original tomogram. The

principle is very similar to random conical tilt (RCT) and orthogonal tilt reconstruction (ORT) tilting concept of taking multiple views and, therefore, it is also referred to as single particle tomography. But the advantage is calculating the structure of a protein or protein complex in situ whereas the challenge is to extract information from a very noisy, crowded and complex environment. Additionally, the sub-volumes are extracted from tomogram at a various orientation which means the orientation of missing wedge also varies accordingly. Therefore, the missing information of one sub-volume in Fourier space is compensated with the sampled region of another sub-volume and the overall missing wedge effect is removed from the final merged image.[68] Therefore, the structures that are calculated using sub-volumes averaging are meaningful and allow to interpret the structure–function relation.

There are two ways to calculate sub-volume averaging: one is multi-reference alignment and classification and the other one is classification by alignment. In multi-reference alignment which is the most used procedure, the sub-tomograms are aligned with respect to a common reference by rotational and translational alignment. Then the aligned particles undergo multivariate data analysis, classification and alignment steps and best classes are selected to be used as references for the next cycle. This iterative procedure runs until the structure no longer changes with subsequent iterations. Finally, the refined transformations are used to generate the final sub-tomogram average.[69] But to reveal the spatial distribution of any macromolecular complex in their physiological environment, the actual orientation of the raw motif has been determined by inverting the calculated rotations and this procedure is known as map-back procedure.[70] With time, the resolution and clarity of original tomogram and sub-tomogram averaged structures steadily improved using new generation microscope, automated data collection for high throughput, sample specific imaging scheme, energy filters, direct detectors and the phase plate. The next section reviews recent developments in the in situ applications of cryo-ET and sub-volume averaging.

Multivariate data analysis: It refers to a statistical method used to observe and analyze data where more than one variable outcome is present.

The field of structural virology has largely benefited from technological advances of the cryo-ET field. Human immunodeficiency virus type I, a pleomorphic virus, difficult to study due to structural heterogeneity and intrinsic flexibility was first viewed in 3D successfully by cryo-ET sub-volume averaging.[71–73] HIV Gag lattice, budding sites, immature virus, CA protein and their change in arrangement during maturation process were thoroughly studied by cryo-ET.[74–78] Envelope (Env) protein of retroviral spikes (including HIV) and their conformational change during interaction with the target cell, interaction with broadly neutralizing antibodies had also caught attention to extract structural information for Env specific vaccine design.[73,79–82] Similarly, another enveloped virus influenza (flu virus) has been studied by several groups to understand entry into a host cell, maturation and budding.[83–86] Figure 8 shows the gallery of few examples of recently solved in situ structures of dynamic biomolecular complexes.

Macromolecular assemblies are the key players in cellular processes to maintain the integrity of the dynamic intracellular architecture. Studies on whole cells (both eukaryotic and prokaryotic) including host–pathogen interactions, cellular organelles have been shown by cryo-ET in unprecedented details in their native environment. Professor Baumeister and colleagues have shown for the first time the disassembly intermediates of vaccinia virus on mammalian cells by whole cell cryo-ET before the resolution revolution era.[92] In the laboratory of Grant Jensen many eukaryotic cells and their organelles, intracellular complexes, bacterial cell ultrastructures including secretion systems were revealed using cryo-ET.[93–97] After phase plate mounted on a TEM as a part of technological advancement and with direct detectors the field of cryo-ET has expanded the boundaries by exploring previously challenged areas.[98–100]

5 Conclusion and Future Directions

Here I have discussed two popular techniques of cryo-EM and their uses in studying a wide range of complexes of macromolecules. Single particle analysis has already achieved a resolution better than 2 Å. With the further advancement and better sample making procedure, it may achieve theoretical resolution in future. Even cryo-ET and sub-tomogram averaging have shown progress and the best resolution of solved structures so far is in the range of 6–8 Å. Applying dose-symmetric tilt scheme in a better-designed microscope there is scope for improvement in resolution. Cryo-ET suffers from resolution limitation mainly due to a thickness of the sample and low SNR. Other than transmission electron microscopic techniques (negative staining and cryo-EM), there are other microscopic techniques (FIB-SEM, Serial Block-face SEM, CLEM) making progress side by side and when applied altogether with cryo-ET drastic improvements occur in understanding dynamic

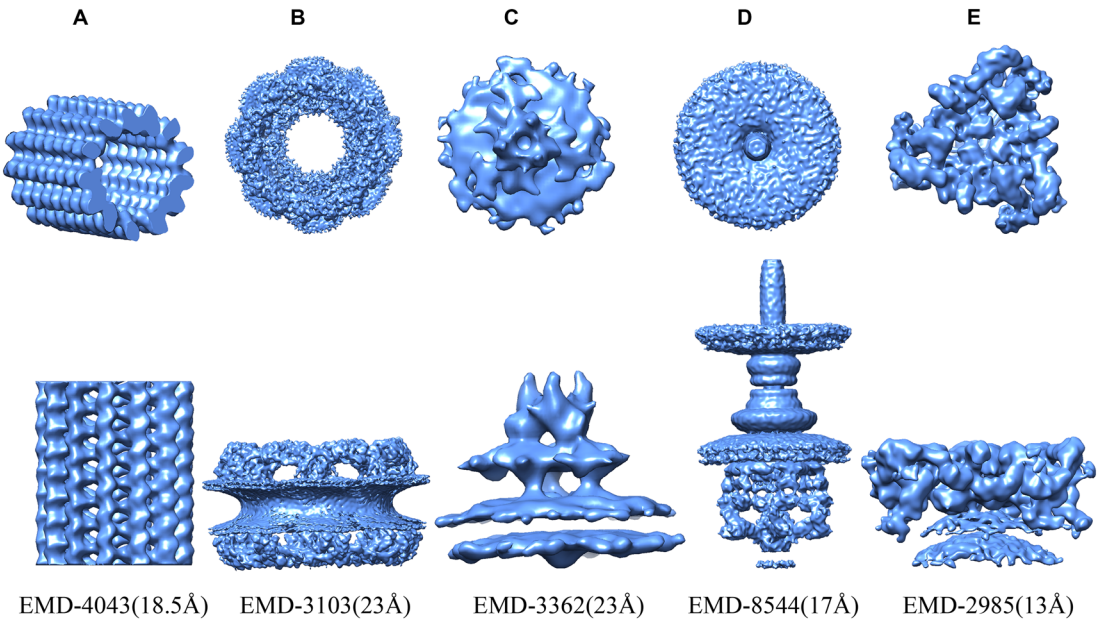

Figure 8: Representative in situ structures of a diverse group of biomolecular complex downloaded from EMDB Data Bank. EM database number and resolution of the reconstruction are indicated below the respective map. First row: Top view and bottom row side view of **a** microtubule,[87] **b** human nuclear pore complex,[88] **c** glycoprotein B HSV 1 [89] **d** injectisome [90] and **e** COPI coat triad [91].

processes of cell biology in unprecedented detail. Cryo-EM has also expanded its functionality in areas such as neuroscience, nano-biotechnology, and pharmaceutical industries. Leaving the world of blobology, cryo-EM has begun studying proteins at molecular detail and yet to explore full potential of this technique in future.

Acknowledgements

I thank Dr. Benjamin Bammes and Dr. Radostin Danev for their approvals to reproduce Figs. 2 and 3, respectively. I thank Dr. Ho Min Kim for his kind permission to reproduce Fig. 5. I am also thankful to Dr. J.J. Fernandez for providing Fig. 7. I thank Dr. Jayati Sengupta for critically reading an earlier version of the manuscript.

Received: 16 April 2018 Accepted: 3 July 2018
Published online: 16 July 2018

References

1. Radermacher M, Wagenknecht T, Verschoor A, Frank J (1987) Three-dimensional reconstruction from a single-exposure, random conical tilt series applied to the 50S ribosomal subunit of *Escherichia coli*. J Microsc 146(Pt 2):113–136
2. Curry Stephen (2015) Structural biology: a century-long journey into an unseen world. Interdisc Sci Rev 40(3):308–328
3. Henderson R, Unwin PN (1975) Three-dimensional model of purple membrane obtained by electron microscopy. Nature 257(5521):28–32
4. De Rosier DJ, Klug A (1968) Reconstruction of three-dimensional structures from electron micrographs. Nature 217:130–134
5. Taylor KA, Glaeser RM (1974) Electron diffraction of frozen, hydrated protein crystals. Science 186:1036–1037
6. Dubochet J, McDowall AW (1981) Vitrification of pure water for electron microscopy. J Microsc 124:RP3–RP4
7. Dubochet J, Adrian M, Chang JJ, Homo JC, Lepault J, McDowall AW, Schultz P (1988) Cryo-electron microscopy of vitrified specimens. Q Rev Biophys 21:129–228
8. Mastronarde D (2003) SerialEM a program for automated tilt series acquisition on Tecnai microscopes using prediction of specimen position. Microsc Microanal 9:1182–1183
9. Suloway C, Pulokas J, Fellmann D, Cheng A, Guerra F, Quispe J, Stagg S, Potter CS, Carragher B (2005) Automated molecular microscopy: the new Leginon system. J Struct Biol 151:41–60
10. Scheres SH (2012) RELION: implementation of a Bayesian approach to cryo-EM structure determination. J Struct Biol 180:519–530
11. Punjani A, Rubinstein JL, Fleet DJ, Brubaker MA (2017) cryoSPARC: algorithms for rapid unsupervised

cryo-EM structure determination. Nat Methods 14(3):290–296
12. Bai XC, Fernandez IS, McMullan G, Scheres SH (2013) Ribosome structures to near atomic resolution from thirty thousand cryo-EM particles. eLife 2:e00461
13. Li X, Mooney P, Zheng S, Booth CR, Braunfeld MB, Gubbens S, Agard DA, Cheng Y (2013) Electron counting and beam-induced motion correction enable near-atomic resolution single-particle cryo-EM. Nat Methods 10(6):584–590
14. Kuhlbrandt W (2014) Biochemistry. The resolution revolution. Science 343(6178):1443–1444
15. Method of the Year 2015 (2016) Nat Methods 13:1
16. Faruqi AR, Henderson R (2007) Electronic detectors for electron microscopy. Curr Opin Struct Biol 17:549–555
17. Zheng SQ, Palovcak E, Armache J, Verba KA, Cheng Y, Agard DA (2017) MotionCor2: anisotropic correction of beam-induced motion for improved cryoelectron microscopy. Nat Methods 14:331–332
18. Brilot AF, Chen JZ, Cheng A, Pan J, Harrison SC, Potter CS, Carragher B, Henderson R, Grigorieff N, Em H (2012) Beam-induced motion of vitrified specimen on holey carbon film. J Struct Biol 177:630–637
19. Zernike F (1942) Phase contrast, a new method for the microscopic observation of transparent objects. Physica 9:686–698
20. Danev R, Nagayama K (2001) Transmission electron microscopy with Zernike phase plate. Ultramicroscopy 88:243–252
21. Danev R, Nagayama K (2008) Single particle analysis based on Zernike phase contrast transmission electron microscopy. J Struc Biol 161:211–218
22. Danev R, Buijsse B, Khoshouei M, Plitzko JM, Baumeister W (2014) potential phase plate for in-focus phase contrast transmission electron microscopy. PNAS (USA) 111:15635–15640
23. Egerton RF (2009) Electron energy-loss spectroscopy in the TEM. Rep Prog Phys 72:16502
24. Schmidt-Krey I, Rubinstein JL (2011) Electron cryomicroscopy of membrane proteins: specimen preparation for two-dimensional crystals and single particles. Micron 42(2):107–116
25. Russo CJ, Passmore LA (2014) Controlling protein adsorption on graphene for cryo-EM using low-energy hydrogen plasmas. Nat Methods 11:649–652
26. Russo CJ, Passmore LA (2014) Ultrastable gold substrates for electron cryomicroscopy. Science 346:1377–1380
27. Dobro MJ, Melanson LA, Jensen GJ, McDowall AW (2010) Plunge freezing for electron cryomicroscopy. Methods Enzymol 481:63–82
28. Mastronarde DN (2005) Automated electron microscope tomography using robust prediction of specimen movements. J Struct Biol 152:36–51
29. Li X, Zheng S, Agard DA, Cheng Y (2015) Asynchronous data acquisition and on-the-fly analysis of dose fractionated cryoEM images by UCSFImage. J Struct Biol 192:174–178
30. Hagen WJH, Wan W, Briggs JAG (2017) Implementation of a cryo-electron tomography tilt-scheme optimized for high resolution subtomogram averaging. J Struct Biol 197:191–198
31. Mahamid J, Baumeister W (2012) Cryo-electron tomography: the realization of a vision. Microsc Microanal 26:45–48
32. Al-Amoudi A, Díez DC, Betts MJ, Frangakis AS (2007) The molecular architecture of cadherins in native epidermal desmosomes. Nature 450(7171):832–837
33. Marko M, Hsieh C, Schalek R, Frank J, Mannella C (2007) Focused-ion-beam thinning of frozen-hydrated biological specimens for cryo-electron microscopy. Nat Methods 4:215–217
34. Kukulski W, Schorb M, Welsch S, Picco A, Kaksonen M, Briggs JAG (2011) Correlated fluorescence and 3D electron microscopy with high sensitivity and spatial precision. JCB 192(1):111–119
35. Hayward SB, Glaeser RM (1979) Radiation damage of purple membrane at low temperature. Ultramicroscopy 04:201–210
36. Downing KH (1988) Observations of restricted beam-induced specimen motion with small-spot illumination. Ultramicroscopy 24:387–397
37. Frank J (1990) Classification of macromolecular assemblies studied as 'single particles'. Q Rev Biophys 23:281–329
38. Frank J (2016) Generalized single-particle cryo-EM—a historical perspective. Microscopy 65(1):3–8
39. Frank J (2017) Advances in the field of single-particle cryo-electron microscopy over the last decade. Nat Protoc 12:209–212
40. Nogales E (2016) The development of cryo-EM into a mainstream structural biology technique. Nat Methods 13(1):24–27
41. Chung J-H, Kim HM (2017) The nobel prize in chemistry 2017: high-resolution cryo-electron microscopy. Appl Microsc 47(4):218–222
42. Jeong H, Lee SG, Kweon HS, Hyun J (2017) Facility for high resolution cryo-electron microscopy of biological macromolecules at Korea Basic Science Institute. Biodesign 5:96–102
43. Frank J (2002) Single-particle imaging of macromolecules by cryo-electron microscopy. Annu Rev Biophys Biomol Struct 31(1):303–319
44. Egelman EH (2010) Reconstruction of helical filaments and tubes. Methods Enzymol 482:167–183
45. Vinothkumar KR (2015) Membrane protein structures without crystals, by single particle electron cryomicroscopy. Curr Opin Struct Biol 33:103–114
46. Rawson S, Davies S, Lippiat JD, Muench SP (2016) The changing landscape of membrane protein structural biology through developments in electron microscopy. Mol Membr Biol 33(1–2):12–22

47. Bartesaghi A, Merk A, Banerjee S, Matthies D, Wu X, Milne JL et al (2015) 2.2 A resolution cryo-EM structure of beta-galactosidase in complex with a cell-permeant inhibitor. Science 348(6239):1147–1151
48. Banerjee S, Bartesaghi A, Merk A, Rao P, Bulfer SL, Yan Y et al (2016) 2.3 A resolution cryo-EM structure of human p97 and mechanism of allosteric inhibition. Science 351(6275):871–875
49. Bai XC, Yan CY, Yang GH, Lu PL, Ma D, Sun LF, Zhou R, Scheres SHW, Shi YG (2015) An atomic structure of human γ-secretase. Nature 525(7568):212–217
50. Liao M, Cao E, Julius D, Cheng Y (2013) Structure of the TRPV1 ion channel determined by electron cryomicroscopy. Nature 504:107–112
51. Merk A, Bartesaghi A, Banerjee S, Falconieri V, Rao P, Davis MI, Pragani R, Boxer MB, Earl LA, Milne JL, Subramaniam S (2016) Breaking cryo-EM resolution barriers to facilitate drug discovery. Cell 165(7):1698–1707
52. Khoshouei M, Danev R, Plitzko JM, Baumeister W (2017) Revisiting the structure of hemoglobin and myoglobin with cryo-electron microscopy. J Mol Biol 429(17):2611–2618
53. Yan C, Hang J, Wan R, Huang M, Wong CC, Shi Y (2015) Structure of a yeast spliceosome at 3.6-angstrom resolution. Science 349:1182–1191
54. Narayanan A, Vago FS, Li K, Qayyum MZ, Yernool D, Jiang W, Murakami KS (2018) Cryo-EM structure of Escherichia coli σ70 RNAP and promoter DNA complex revealed a role of σ nonconserved region during the open complex formation. J Biol Chem 293(19):7367–7375
55. Scapin G, Dandey VP, Zhang Z, Prosise W, Hruza A, Kelly T, Mayhood T, Strickland C, Potter CS, Carragher B (2018) Structure of the insulin receptor-insulin complex by single-particle cryo-EM analysis. Nature 556:122–125
56. Vinothkumar KR, Zhu J, Hirst J (2014) Architecture of mammalian respiratory complex I. Nature 515(7525):80–84
57. Henderson R, Sali A, Baker ML, Carragher B, Devkota B, Downing KH, Egelman EH, Feng Z, Frank J, Grigorieff N et al (2012) Outcome of the first electron microscopy validation task force meeting. Structure 20:205–214
58. Villa E, Lasker K (2014) Finding the right fit: chiseling structures out of cryo-electron microscopy maps. Curr Opin Struct Biol 25:118–125
59. Rosenthal PB, Henderson R (2003) Optimal determination of particle orientation, absolute hand, and contrast loss in single-particle electron cryomicroscopy. J Mol Biol 333:721–745
60. Galaz-Montoya JG, Ludtke SJ (2017) The advent of structural biology in situ by single particle cryoelectron tomography. Biophys Rep 3(1–3):17–35
61. Fernandez JJ (2012) Computational methods for electron tomography. Micron 43:1010–1030
62. Kremer JR, Mastronarde DN, McIntosh JR (1996) Computer visualization of three-dimensional image data using IMOD. J Struct Biol 116(1):71–76
63. Winkler H, Taylor KA (2006) Accurate marker-free alignment with simultaneous geometry determination and reconstruction of tilt series in electron tomography. Ultramicroscopy 106(3):240–254
64. Liu Y, Penczek PA, McEwen BF, Frank J (1995) A marker-free alignment method for electron tomography. Ultramicroscopy 58(3):393–402
65. Winkler H, Taylor KA (2003) Focus gradient correction applied to tilt series image data used in electron tomography. J Struct Biol 143(1):24–32
66. Zanetti G, Riches JD, Fuller SD, Briggs JA (2009) Contrast transfer function correction applied to cryo-electron tomography and sub-tomogram averaging. J Struct Biol 168(2):305–312
67. Schur FK, Hagen W, de Marco A, Briggs JA (2013) Determination of protein structure at 8.5 Å resolution using cryo-electron tomography and subtomogram averaging. J Struct Biol 184(3):394–400
68. Liu J, Wright ER, Winkler H (2010) 3D visualization of HIV virions by cryoelectron tomography. Methods Enzymol 483:267–290
69. Winkler H, Zhu P, Liu J, Ye F, Roux KH, Taylor KA (2009) Tomographic subvolume alignment and subvolume classification applied to myosinV and SIV envelope spikes. J Struct Biol 165(2):64–77
70. Liu J, Reedy MC, Goldman YE, Franzini-Armstrong C, Sasaki H, Tregear RT, Lucaveche C, Winkler H, Baumann BAJ, Squire JM, Irving TC, Reedy MK, Taylor KA (2004) Electron tomography of fast frozen, stretched rigor fibers reveals elastic distortions in the myosin crossbridges. J Struct Biol 147(3):268–282
71. Zhu P, Liu J, Bess J Jr, Chertova E, Lifson JD, Grise H, Ofek GA, Taylor KA, Roux KH (2006) Distribution and three-dimensional structure of AIDS virus envelope spikes. Nature 441:847–852
72. Zanetti G, Briggs JA, Grunewald K, Sattentau QJ, Fuller SD (2006) Cryo-electron tomographic structure of an immunodeficiency virus envelope complex in situ. PLoS Pathog 2:83
73. Liu J, Bartesaghi A, Borgnia MJ, Sapiro G, Subramaniam S (2008) Molecular architecture of native HIV-1 gp120 trimers. Nature 455:109–113
74. Wright ER, Schooler JB, Ding HJ, Kieffer C, Fillmore C, Sundquist WI, Jensen GJ (2007) Electron cryotomography of immature HIV-1 virions reveals the structure of the CA and SP1 Gag shells. EMBO J 26:2218–2226
75. Briggs JA, Riches JD, Glass B, Bartonova V, Zanetti G, Krausslich HG (2009) Structure and assembly of immature HIV. Proc Natl Acad Sci USA 106:11090–11095
76. de Marco A, Müller B, Glass B, Riches JD, Kräusslich HG, Briggs JAG (2010) Structural analysis of HIV-1 maturation using cryo-electron tomography. PLoS Pathog 6(11):e1001215
77. Bharat TA, Davey NE, Ulbrich P, Riches JD, de Marco A, Rumlova M, Sachse C, Ruml T, Briggs JA (2012) Structure of the immature retroviral capsid at 8 Å resolution

by cryo-electron microscopy. Nature 487(7407):385–389. https://doi.org/10.1038/nature11169

78. Schur FK, Hagen WJ, Rumlová M, Ruml T, Müller B, Kräusslich HG, Briggs JA (2015) Structure of the immature HIV-1 capsid in intact virus particles at 8.8 Å resolution. Nature 517(7535):505–508. https://doi.org/10.1038/nature13838 **(Epub 2014 Nov 2)**
79. White TA, Bartesaghi A, Borgnia MJ et al (2010) Molecular architectures of trimeric SIV and HIV-1 envelope glycoproteins on intact viruses: strain-dependent variation in quaternary structure. PLoS Pathog 6(12):e1001249
80. White TA, Bartesaghi A, Borgnia MJ et al (2011) Three-dimensional structures of soluble CD4-bound states of trimeric simian immunodeficiency virus envelope glycoproteins determined by using cryo-electron tomography. J Virol 85(23):12114–12123. https://doi.org/10.1128/JVI.05297-11
81. Tran EEH, Borgnia MJ, Kuybeda O et al (2012) structural mechanism of trimeric HIV-1 envelope glycoprotein activation. PLoS Pathog 8(7):e1002797. https://doi.org/10.1371/journal.ppat.1002797
82. Dutta M, Liu J, Roux KH, Taylor KA (2014) Visualization of retroviral envelope spikes in complex with the V3 loop antibody 447-52D on intact viruses by cryo-electron tomography. J Virol 88(21):12265–12275. https://doi.org/10.1128/JVI.01596-14
83. Fontana J, Steven AC (2013) At low pH, influenza virus matrix protein M1 undergoes a conformational change prior to dissociating from the membrane. J Virol 87(10):5621–5628
84. Chlanda P, Schraidt O, Kummer S, Riches J, Oberwinkler H, Prinz S, Briggs JAG (2015) Structural analysis of the roles of influenza A virus membrane-associated proteins in assembly and morphology. J Virol 89(17):8957–8966
85. Gui L, Ebner JL, Mileant A, Williams JA, Lee KK (2016) Visualization and sequencing of membrane remodeling leading to influenza virus fusion. J Virol 90(15):6948–6962
86. Calder LJ, Rosenthal PB (2016) Cryomicroscopy provides structural snapshots of influenza virus membrane fusion. Nat Struct Mol Biol 23(9):853–858
87. Grange M, Vasishtan D, Grünewald K (2017) Cellular electron cryo tomography and in situ sub-volume averaging reveal the context of microtubule-based processes. J Struct Biol 197(2):181–190
88. von Appen A, Kosinski J, Sparks L, Ori A, DiGuilio A, Vollmer B, Mackmull M, Banterle N, Parca L, Kastritis P, Buczak K, Mosalaganti S, Hagen W, Andres-Pons A, Lemke EA, Bork P, Antonin W, Glavy JS, Bui KH, Beck M (2015) In situ structural analysis of the human nuclear pore complex. Nature 526:140–143
89. Zeev-Ben-Mordehai T, Vasishtan D, Hernández Durán A, Vollmer B, White P, Pandurangan AP, Siebert CA, Topf M, Grünewald K (2016) Two distinct trimeric conformations of natively membrane-anchored full-length herpes simplex virus 1 glycoprotein B. Proc Natl Acad Sci USA 113(15):4176–4181
90. Hu B, Lara-Tejero M, Kong Q, Galan JE, Liu J (2017) In situ molecular architecture of the salmonella type III secretion machine. Cell 168:1065–1074
91. Dodonova SO, Diestelkoetter-Bachert P, von Appen A, Hagen WJH, Beck R, Beck M, Wieland F, Briggs JAG (2015) A structure of the COPI coat and the role of coat proteins in membrane vesicle assembly. Science 349(6244):195–198
92. Cyrklaff M, Linaroudis A, Boicu M et al (2007) Whole cell cryo-electron tomography reveals distinct disassembly intermediates of vaccinia virus. PLoS ONE 2(5):e420. https://doi.org/10.1371/journal.pone.0000420
93. Swulius MT, Chen S, Ding HJ et al (2011) Long helical filaments are not seen encircling cells in electron cryotomograms of rod-shaped bacteria. Biochem Biophys Res Commun 407(4):650–655. https://doi.org/10.1016/j.bbrc.2011.03.062
94. Pilhofer M et al (2013) Discovery of chlamydial peptidoglycan reveals bacteria with murein sacculi but without FtsZ. Nat Commun 4:2856. https://doi.org/10.1038/ncomms3856
95. Abrusci P, Vergara-Irigaray M, Johnson S et al (2013) Architecture of the major component of the type III secretion system export apparatus. Nat Struct Mol Biol 20(1):99–104. https://doi.org/10.1038/nsmb.2452
96. Müller A, Beeby M, McDowall AW, Chow J, Jensen GJ, Clemons WM (2014) Ultrastructure and complex polar architecture of the human pathogen *Campylobacter jejuni*. Microbiol Open 3(5):702–710. https://doi.org/10.1002/mbo3.200
97. Oikonomou CM, Jensen GJ (2016) A new view into prokaryotic cell biology from electron cryotomography. Nat Rev Microbiol 14(4):205–220. https://doi.org/10.1038/nrmicro.2016.7
98. Fukuda Y, Laugks U, Lučić V, Baumeister W, Danev R (2015) Electron cryotomography of vitrified cells with a Volta phase plate. J Struct Biol 190(2):143–154. https://doi.org/10.1016/j.jsb.2015.03.004 **(Epub 2015 Mar 12)**
99. Mahamid J, Pfeffer S, Schaffer M, Villa E, Danev R, Cuellar LK, Förster F, Hyman AA, Plitzko JM, Baumeister W (2016) Visualizing the molecular sociology at the HeLa cell nuclear periphery. Science 351(6276):969–972. https://doi.org/10.1126/science.aad8857
100. Sharp TH, Faas FGA, Koster AJ, Gros P (2017) Imaging complement by phase-plate cryo-electron tomography from initiation to pore formation. J Struct Biol 197(2):155–162. https://doi.org/10.1016/j.jsb.2016.09.008 **(Epub 2016 Sep 20)**

Moumita Dutta Dr. Moumita Dutta working as Scientist C (EM Division) at ICMR-National Institute of Cholera and Enteric Diseases, Kolkata. She had completed her B.Sc in Chemistry (Hons) from University of Calcutta, M.Sc in Biochemistry from University of Calcutta and Ph.D. in Life Sciences and Biotechnology from NICED affiliated to Jadavpur University. She moved to the USA as a Postdoctoral Fellow at Florida State University to study HIV/SIV glycoprotein spikes and their complexes with broadly neutralizing antibodies using cryo-electron tomography and sub-tomogram averaging to provide structural information for designing better immunogen. Later, she moved to MRC-NIMR, London (part of The Francis Crick Institute, London, UK) as a career development fellow to work on structural intermediates of bacterial replication initiation process and also retroviral capsid structures using cryo-electron tomography. Later, she had worked as a senior staff scientist in cryo-electron microscopy at University of Sheffield, Sheffield, UK.